

**Cooling-field dependence of exchange bias effect in La<sub>0.45</sub>Sr<sub>0.55</sub>MnO<sub>3</sub> nanoparticles**

A. Rostamnejadi, M. Venkatesan, P. Kameli, H. Salamati, and J. M. D. Coey

Citation: *Journal of Applied Physics* **116**, 043913 (2014); doi: 10.1063/1.4890723

View online: <http://dx.doi.org/10.1063/1.4890723>

View Table of Contents: <http://scitation.aip.org/content/aip/journal/jap/116/4?ver=pdfcov>

Published by the [AIP Publishing](#)

---

**Articles you may be interested in**

[Tunable magnetic and magnetocaloric properties of La<sub>0.6</sub>Sr<sub>0.4</sub>MnO<sub>3</sub> nanoparticles](#)

*J. Appl. Phys.* **114**, 223907 (2013); 10.1063/1.4846758

[Exchange bias in La<sub>0.7</sub>Sr<sub>0.3</sub>MnO<sub>3</sub>/NiO and LaMnO<sub>3</sub>/NiO interfaces](#)

*J. Appl. Phys.* **113**, 223903 (2013); 10.1063/1.4811227

[A study of exchange bias in BiFeO<sub>3</sub> core/NiFe<sub>2</sub>O<sub>4</sub> shell nanoparticles](#)

*J. Appl. Phys.* **113**, 173906 (2013); 10.1063/1.4803549

[Conventional and inverse magnetocaloric effects in La<sub>0.45</sub>Sr<sub>0.55</sub>MnO<sub>3</sub> nanoparticles](#)

*J. Appl. Phys.* **110**, 043905 (2011); 10.1063/1.3614586

[Tunneling magnetoresistance in spin valves exchange biased with metallic antiferromagnet La<sub>0.45</sub>Sr<sub>0.55</sub>MnO<sub>3</sub>](#)




*J. Appl. Phys.* **106**, 103924 (2009); 10.1063/1.3260247

---



**AIP** | Journal of Applied Physics

**Meet The New Deputy Editors**

	<b>Christian Brosseau</b>		<b>Laurie McNeil</b>		<b>Simon Phillpot</b>
---	---------------------------	---	----------------------	---	-----------------------

# Cooling-field dependence of exchange bias effect in $\text{La}_{0.45}\text{Sr}_{0.55}\text{MnO}_3$ nanoparticles

A. Rostamnejadi,<sup>1,2,a)</sup> M. Venkatesan,<sup>2</sup> P. Kameli,<sup>1</sup> H. Salamati,<sup>1</sup> and J. M. D. Coey<sup>2</sup>

<sup>1</sup>Department of Physics, Isfahan University of Technology, Isfahan 84156-83111, Iran

<sup>2</sup>CRANN and School of Physics, Trinity College, Dublin 2, Ireland

(Received 29 May 2014; accepted 9 July 2014; published online 28 July 2014)

Magnetic properties of 16 nm  $\text{La}_{0.45}\text{Sr}_{0.55}\text{MnO}_3$  nanoparticles exhibit superparamagnetic blocking at 160 K with a ferromagnetic moment appearing in the antiferromagnetic state. The exchange interaction at the interface between canted ferromagnetic and antiferromagnetic regions within the nanoparticles leads to exchange bias, but the loop shift, coercivity, and remanence asymmetry all decrease strongly with increasing cooling field above 1 T unlike a conventional ferromagnetic/antiferromagnetic exchange bias system. The observations imply a magnetization process involving coalescence of canted ferromagnetic clusters with increasing field, which reduces the interface area with the antiferromagnetic matrix. © 2014 AIP Publishing LLC. [<http://dx.doi.org/10.1063/1.4890723>]

## I. INTRODUCTION

Doped perovskite manganites have been a focus of intensive study ever since the discovery of colossal magnetoresistance, on account of their complex physics and potential applications.<sup>1</sup> Several experimental reports show that potentially charge-ordered antiferromagnetic (AFM) manganites behave differently in the bulk and in nanoparticle form.<sup>2–8</sup> For example, the charge ordered, antiferromagnetic state in  $\text{La}_{0.5}\text{Ca}_{0.5}\text{MnO}_3$  nanoparticles may be suppressed, leaving a ferromagnetic (FM) state with a reduced moment.<sup>4,7</sup> The mechanism for stabilization of ferromagnetism is a topic for debate, but suggestions include surface effects (core/shell models),<sup>2,3,9,10</sup> surface hydrostatic pressure,<sup>7</sup> and intrinsic structural distortions.<sup>8</sup>

Exchange coupling at an AFM/FM interface tends to induce unidirectional exchange anisotropy when the sample is cooled through the Néel temperature of the AFM component in the presence of static magnetic field.<sup>11,12</sup> The exchange anisotropy causes a shift in the magnetic hysteresis loop which is known as exchange bias (EB).<sup>12</sup> Recently, EB has been found in manganites that are phase separated<sup>13,14</sup> or cluster spin-glass-like,<sup>15</sup> and in nanoparticles<sup>3,16,17</sup> or AFM/FM manganite thin film structures.<sup>18,19</sup>

While many studies are focused on half-doped, charged-ordered AFM manganites, there is no systematic study of the magnetic properties of  $\text{La}_{1-x}\text{Sr}_x\text{MnO}_3$  nanoparticles for  $x > 0.5$ . In this letter, we present unusual ferromagnetic properties and exchange bias in  $\text{La}_{0.45}\text{Sr}_{0.55}\text{MnO}_3$  (LSMO) nanoparticles. Both DC magnetization and AC magnetic susceptibility measurements show the existence of a disordered magnetic state with a net ferromagnetic moment at low temperature. The effect of cooling field (CF) on the loop shift, coercivity, and remanence asymmetry at 5 K has been investigated. The magnitude of the EB field decreases strongly with increasing CF, which is in contrast with the behaviour of conventional FM/AFM EB systems.

## II. EXPERIMENTS

Nanoparticles of LSMO were prepared by a sol-gel method.<sup>20</sup> The X-Ray diffraction analysis confirms that the samples are single phase with no detectable secondary phases; the crystal structure is tetragonal with space group  $I4/mcm$ . Transmission electron microscopy (TEM) shows a nearly homogeneous particle size distribution; high resolution TEM confirms the crystalline nature of the nanoparticles. Magnetic properties were studied using a Quantum Design MPMS 5 T SQUID magnetometer and an AC magnetic susceptometer (Lake Shore, model 7000). The magnetization at 5 K first increases with particle size from  $1.0 \mu_B/\text{Mn}$  for 16 nm to  $1.5 \mu_B/\text{Mn}$  for 36 nm before falling abruptly in larger particles,<sup>21</sup> which have an A-type antiferromagnetic spin structure.<sup>22</sup> We focus on the particles with  $2r = 16$  nm.

## III. RESULTS AND DISCUSSION

Figure 1(a) shows the temperature dependence of magnetization of the 16 nm particles, in zero field cooled (ZFC) and field cooled (FC) modes in applied fields of 5, 50, and 500 mT. The Curie temperature of the sample is close to room temperature. The ZFC and FC curves bifurcate upon decreasing temperature in a field that is considerably greater than the coercivity at that temperature, indicating the onset of a magnetization blocking process. The blocking temperature ( $T_B$ ) decreases with increasing magnetic field due to its stabilizing effect on the ferromagnetic moment. The FC magnetization of the sample increases with decreasing temperature below  $T_B$ , which is normal for a superparamagnetic systems.<sup>23</sup> The temperature dependence of the AC magnetic susceptibility  $\chi'(T)$  around  $T_B$ , which is depicted in Fig. 1(b), shows a peak which is frequency dependent and shifts to higher temperature on increasing frequency. This is also a superparamagnetic characteristic.<sup>20</sup> Unlike single crystal and bulk samples of LSMO,<sup>24–26</sup> no FM-AFM transition is detected in the FC magnetization curve of the sample. The nanoparticles do not have a simple antiferromagnetic ground state.

<sup>a)</sup>Author to whom correspondence should be addressed. Electronic mail: arostamnejadi@gmail.com

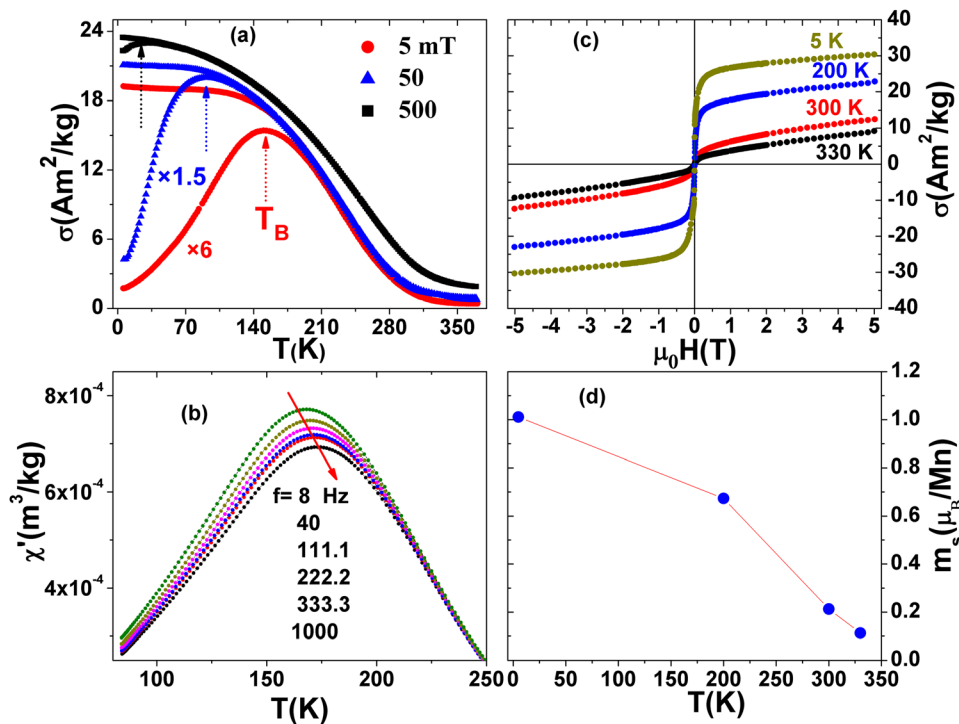


FIG. 1. (a) ZFC and FC magnetization of the sample as a function of temperature in 5, 50, and 500 mT. (b) AC magnetic susceptibility versus T. (c) Magnetization of the sample at 5, 200, 300, and 330 K. (d) Saturation magnetic moment of the sample as a function of temperature.

Figure 1(c) shows the magnetization of the sample at different temperatures. It should be noted that it is far from saturated even in 5 T and varies almost linearly with magnetic field for  $\mu_0 H > 1$  T, suggesting that the ferromagnetism is due to spin canting in an underlying antiferromagnetic structure. Collinear saturation would need an extrapolated field of 70 T, which gives the order of magnitude of the antiferromagnetic exchange coupling. The saturation magnetic moment,  $m_s$ , of the manganese versus temperatures is shown in Fig. 1(d) where it is seen to increase on decreasing temperature reaching the value of  $1.0 \mu_B/\text{Mn}$  at 5 K, just 29% of the  $3.45 \mu_B/\text{Mn}$ , expected for a collinear ferromagnetic structure, but much higher than the values reported for bulk and single crystal of LSMO.<sup>24–26</sup> If the ferromagnetism was completely concentrated in the core of the particle, the core would have a diameter of 10.4 nm, but if there was a collinear ferromagnetic outer shell, it would have a thickness of 0.9 nm.

The magnetic properties of mixed-valence manganites are usually described in terms of competing double exchange (DE) and super exchange (SE) interactions.<sup>1</sup> In bulk tetragonal manganites with  $x \geq 0.5$ , the DE interaction mediates ferromagnetic coupling between  $\text{Mn}^{3+}$  and  $\text{Mn}^{4+}$  ions within the  $ab$  plane and the SE interaction produces out of plane antiferromagnetic coupling along the  $c$  axis, resulting in the A-type antiferromagnetic ground state.<sup>24,25</sup> A canted ferromagnetic structure with a net moment  $\leq 1 \mu_B/\text{Mn}$  has slightly higher energy, but it can be stabilized by entropy if the canting is random. However, the antiferromagnetic state becomes increasingly unstable in small particles compared to the canted state. Since the surface/volume ratio increases as  $1/r$ , it might be reasonable to model the nanoparticles in terms of an antiferromagnetic core and a canted, ferromagnetic outer magnetic shell, as shown in Fig. 2(a). The observed moment is much too large to explain by truncation

of the A-type antiferromagnetic structure by the nanoparticle surface. The conduction electrons may tend to be localized at the surface of nanoparticles because of band narrowing and the possibility of unconstrained Jahn-Teller distortion of the coordination shell of  $\text{Mn}^{3+}$ . The spin structure would therefore tend to be more disordered in the outer shell than in the deeper layers, where DE is active. An alternative model of the magnetic nanoparticle is a more uniform randomly-canted state with a reduced net moment, and local spatial fluctuations of the magnetization, as illustrated in Fig. 2(b). The nanoparticle contains small canted ferromagnetic clusters in an antiferromagnetic matrix.

To test the models, we have measured the hysteresis loop of the sample at 5 K in both the ZFC and FC states. For the ZFC mode, the sample was cooled in zero field from 300 K to 5 K. For the FC process, the sample was cooled in  $\pm 5$  T magnetic field. Then, the saturated hysteresis loops

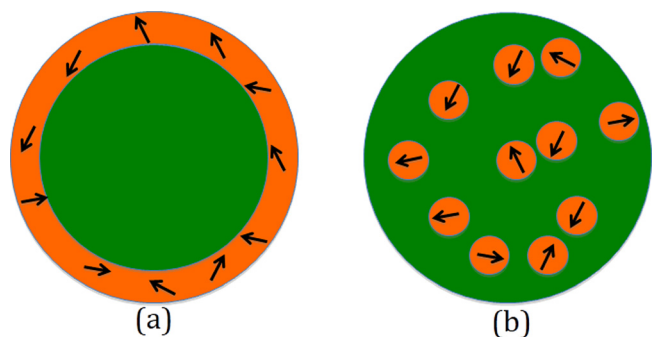


FIG. 2. Model magnetic structures of a LSMO nanoparticle. (a) A core/shell model with an antiferromagnetic core (green) and a canted ferromagnetic shell (orange). Exchange bias arises at the core-shell interface. (b) A cake/corral model with canted ferromagnetic clusters (orange) embedded in an antiferromagnetic matrix (green). The zero-field cooled structure is illustrated. The high-field magnetization process involves coalescence of clusters with aligned ferromagnetic moments.

were measured between  $\pm 5$  T. It can be seen in Fig. 3(a) that the ZFC magnetization shows a symmetric hysteresis loop with coercivity and remanence of 45 mT and  $9.5 \text{ A m}^2 \text{ kg}^{-1}$ , respectively. The FC loops show asymmetry, exhibiting a shift along both the field and magnetization axes. Coercivity is enhanced in both  $+5$  T and  $-5$  T FC loops compared to that in ZFC loop. The EB and coercive fields are defined as  $H_{EB} = (H_2 + H_1)/2$  and  $H_C = (H_2 - H_1)/2$ , where  $H_1$  and  $H_2$  are the negative and positive coercivity, respectively. Remanence asymmetry and remanence, which correspond to  $H_{EB}$  and  $H_C$ ,<sup>13</sup> are defined as  $\sigma_{EB} = (\sigma_1 + \sigma_2)/2$  and  $\sigma_C = (\sigma_1 - \sigma_2)/2$ , respectively, where  $\sigma_1$  and  $\sigma_2$  are the positive and negative remanence, respectively. The values obtained for  $\mu_0 H_{EB}$ ,  $\mu_0 H_C$  and  $\sigma_{EB}$  from the FC loops with magnetic fields (5 T,  $-5$  T) are ( $-18.9$  mT,  $18.9$  mT), ( $59.0$  mT,  $59.7$  mT), and ( $2.0 \text{ A m}^2 \text{ kg}^{-1}$ ,  $-2.0 \text{ A m}^2 \text{ kg}^{-1}$ ), respectively. These values confirm the existence of EB in LSMO nanoparticles and its homogeneity under positive and negative FC processes. The value of  $H_{EB}$  exceeds that reported for the thin film bilayers  $\text{La}_{0.67}\text{Sr}_{0.33}\text{MnO}_3/\text{La}_{0.45}\text{Sr}_{0.55}\text{MnO}_3$ .<sup>18</sup>

In the ZFC process for the structures of Fig. 2, the magnetization of the partly ferromagnetic shell or clusters orients with the field, but at random relative to the antiferromagnetic cores of the nanoparticles. The exchange anisotropy is averaged out, and the ZFC loop does not shift. In the FC process, the ferromagnetic moment orients in the direction of the cooling field. Below the freezing temperature, the disordered interfacial spins are frozen with some of them aligned in directions determined by the field. When the measuring field is inverted, the FM spins start to rotate, but the interface spins can remain unchanged. The interface interaction exerts a microscopic torque on the FM spins and tries to keep them in their original orientation. Therefore a larger magnetic field is necessary to rotate the FM spins and the hysteresis loop shifts.

In the core/shell model of Fig. 2(a), the size of the AF core should be practically independent of magnetic field, since the magnetization changes only slightly in 5 T, Fig. 1(c). The interface area remains practically constant, so the system resembles the standard AF/FM exchange bias bilayer.

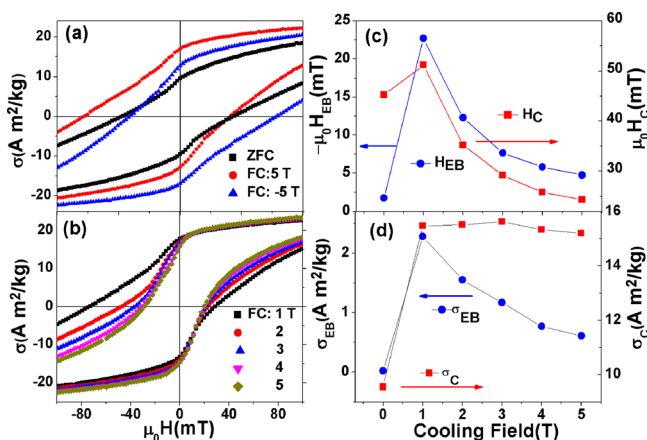


FIG. 3. (a) ZFC and FC magnetization hysteresis loops of the sample at 5 K. Cooling field dependence of (b) the hysteresis loop, (c)  $H_{EB}$  and  $H_C$ , (d)  $\sigma_{EB}$  and  $\sigma_C$  at 5 K.

The EB is then expected to *increase* with cooling field, in the normal way.<sup>12</sup>

Figure 3(b) shows the FC hysteresis loops of the sample recorded at 5 K with successive cooling at 1 T to 5 T. The variation of  $H_{EB}$ ,  $H_C$ ,  $\sigma_E$  and  $\sigma_C$  are plotted as a function of cooling field in Figs. 3(c) and 3(d). A strong *decrease* in both  $H_{EB}$  and  $H_C$  is observed, in contrast to standard FM/AFM systems.<sup>27</sup> In our case, the EB varies inversely with cooling field in the range 1–5 T so that

$$\mu_0(H_{EB}H_{CF})^{1/2} \approx 152 \text{ mT}. \quad (1)$$

It can be noted that the vertical loop shift  $\sigma_{EB}$  also decreases with cooling field whereas the average remanence  $\sigma_C$  at 5 K is nearly constant at  $15 \text{ A m}^2 \text{ kg}^{-1}$ , which is about half the saturation magnetization, Fig. 1(c).

In a standard FM/AFM bilayer, the magnitude of  $H_{EB}$  is given by<sup>12</sup>

$$H_{EB} = \varepsilon_{ex}/\mu_0 M_s t_F, \quad (2)$$

where  $\varepsilon_{ex}$  is the interfacial coupling energy,  $M_s$  and  $t_F$  are the saturation magnetization and thickness of the FM layer, respectively. The thickness of the antiferromagnetic layer should exceed a threshold value, and EB then falls off as the inverse of the ferromagnetic layer thickness. In a  $\text{La}_{0.45}\text{Sr}_{0.55}\text{MnO}_3$  (80 nm)/ $\text{La}_{0.67}\text{Sr}_{0.33}\text{MnO}_3$  (80 nm) bilayer,  $\varepsilon_{ex}$  was found to be  $0.13 \text{ mJ/m}^2$  at 10 K.<sup>18</sup> The value of  $\varepsilon_{ex}$  deduced from the core/shell model of Fig. 2(a) based on the value of  $H_{EB}$  obtained in 1 T is an order of magnitude smaller,  $0.008 \text{ mJ/m}^2$ . This value is not much altered if a thicker ferromagnetic surface layer with canted spins is involved, since it is the product  $M_s t_F$  that appears in Eq. (2).

The core/shell model of Fig. 2(a) does not explain the five-fold decrease of  $H_{EB}$  when the field is increased from 1 to 5 T. Obviously, the high-field magnetization process has the effect of destroying the exchange bias in the nanoparticles. This can be understood with the cake/currant cluster model of Fig. 2(b), if the magnetization process involves coalescence of the canted, ferromagnetic clusters. The exchange bias is proportional to the interface area, which decreases as the clusters coalesce. If the ferromagnetic volume  $V$  is divided into  $n$  spherical clusters, the EB field

$$H_{EB} = (3\varepsilon_{ex}/\mu_0 M)(4\pi n/3V)^{1/3} \sim n^{1/3}, \quad (3)$$

where  $M$  is the magnetization of the ferromagnetic regions. The decrease of  $H_{EB}$  is associated with a 100 fold decrease in  $n$ , from many clusters having  $\sim 100$  atoms in the 1 T FC state to only a few large clusters in the 16 nm nanoparticles in the 5 T FC state. The value of  $\varepsilon_{ex}$  is therefore approximately  $0.01 \text{ mJ/m}^2$ . The decrease of  $H_{EB}$  by CF is also consistent with Monte Carlo simulation and experimental results of EB systems having a spin glass component.<sup>14,15,27–29</sup>

#### IV. CONCLUSIONS

In conclusion, we find a relatively strong FM moment at low temperatures ( $\approx 1.0 \mu_B/\text{Mn}$ ) in 16 nm LSMO nanoparticles, unlike that observed in single crystals and bulk

polycrystalline LSMO. Local disorder and surface effects change the competition between double exchange and super-exchange interactions; consequently randomly oriented canted ferromagnetic regions form in an underlying antiferromagnetic state. Two models are considered for the spin structure of the nanoparticles, but only the cake/currant model with many small ferromagnetic clusters in the antiferromagnetic matrix of a nanoparticle is consistent with the strong decrease in EB observed with increasing CF. The exchange interaction at the interfaces of the canted ferromagnetic regions induces unidirectional anisotropy and leads to the loop shift. In large cooling fields, the interface area between ferromagnetic and antiferromagnetic regions decreases as the cluster coalesces, thereby weakening the EB.

## ACKNOWLEDGMENTS

This work was supported by Science Foundation Ireland as part of the MANSE project 05/IN/1850 and the NISE project 10/IN1/I3002.

- <sup>1</sup>J. M. D. Coey, M. Viret, and S. Von Molnar, *Adv. Phys.* **58**, 571 (2009).
- <sup>2</sup>C. Lu, S. Dong, K. Wang, F. Gao, P. Li, L. Lv, and J. M. Liu, *Appl. Phys. Lett.* **91**, 032502 (2007).
- <sup>3</sup>S. Zhou, L. Shi, H. Yang, Y. Wang, L. He, and J. Zhao, *Appl. Phys. Lett.* **93**, 182509 (2008).
- <sup>4</sup>Jirak, Z., Hadov, E., O. Kaman, Knizek, K., M. Marysko, E. Pollert, M. Dlouha, and S. Vratislav, *Phys. Rev. B* **81**, 024403 (2010).
- <sup>5</sup>S. Rao, K. Anuradha, S. Sarangi, and S. Bhat, *Appl. Phys. Lett.* **87**, 182503 (2005).
- <sup>6</sup>S. S. Rao, S. Tripathi, D. Pandey, and S. V. Bhat, *Phys. Rev. B* **74**, 144416 (2006).
- <sup>7</sup>T. Sarkar, B. Ghosh, A. K. Raychaudhuri, and T. Chatterji, *Phys. Rev. B* **77**, 235112 (2008).
- <sup>8</sup>Y. Wang and H. J. Fan, *Appl. Phys. Lett.* **98**, 142502 (2011).
- <sup>9</sup>S. Dong, F. Gao, Z. Wang, J. M. Liu, and Z. Ren, *Appl. Phys. Lett.* **90**, 082508 (2007).
- <sup>10</sup>S. Dong, R. Yu, S. Yunoki, J. M. Liu, and E. Dagotto, *Phys. Rev. B* **78**, 064414 (2008).
- <sup>11</sup>W. Meiklejohn and C. Bean, *Phys. Rev.* **105**, 904 (1957).
- <sup>12</sup>J. Nogués, J. Sort, V. Langlais, V. Skumryev, S. Suriñach, J. S. Muñoz, and M. D. Baró, *Phys. Rep.* **422**, 65 (2005).
- <sup>13</sup>D. Niebieskikwiat and M. Salamon, *Phys. Rev. B* **72**, 174422 (2005).
- <sup>14</sup>T. Qian, G. Li, T. Zhang, T. Zhou, X. Xiang, X. Kang, and X. Li, *Appl. Phys. Lett.* **90**, 012503 (2007).
- <sup>15</sup>S. Karmakar, S. Taran, E. Bose, B. Chaudhuri, C. Sun, C. Huang, and H. Yang, *Phys. Rev. B* **77**, 144409 (2008).
- <sup>16</sup>T. Zhang and M. Dressel, *Phys. Rev. B* **80**, 014435 (2009).
- <sup>17</sup>S. Zhou, S. Zhao, Y. Guo, J. Zhao, and L. Shi, *J. Appl. Phys.* **107**, 033906 (2010).
- <sup>18</sup>P. Muduli and R. Budhani, *Appl. Phys. Lett.* **94**, 202510 (2009).
- <sup>19</sup>A. L. Kobrinskii, A. M. Goldman, M. Varela, and S. J. Pennycook, *Phys. Rev. B* **79**, 094405 (2009).
- <sup>20</sup>A. Rostamnejadi, H. Salamati, P. Kameli, and H. Ahmadvand, *J. Magn. Mater.* **321**, 3126 (2009).
- <sup>21</sup>A. Rostamnejadi, M. Venkatesan, J. Alaria, M. Boese, P. Kameli, H. Salamati, and J. Coey, *J. Appl. Phys.* **110**, 043905 (2011).
- <sup>22</sup>S. J. May, P. Ryan, J. Robertson, J. W. Kim, T. S. Santos, E. Karapetrova, J. L. Zarestky, X. Zhai, S. Te Velthuis, and J. Eckstein, *Nat. Mater.* **8**, 892–897 (2009).
- <sup>23</sup>D. Parker, F. Ladieu, E. Vincent, G. Méridet, E. Dubois, V. Dupuis, and R. Perzynski, *J. Appl. Phys.* **97**, 10A502 (2005).
- <sup>24</sup>O. Chmaissem, B. Dabrowski, S. Kolesnik, J. Mais, J. D. Jorgensen, and S. Short, *Phys. Rev. B* **67**, 094431 (2003).
- <sup>25</sup>J. Hemberger, A. Krimmel, T. Kurz, H. A. K. von Nidda, V. Y. Ivanov, A. Mukhin, A. Balbashov, and A. Loidl, *Phys. Rev. B* **66**, 094410 (2002).
- <sup>26</sup>A. Szewczyk, M. Gutowska, and B. Dabrowski, *Phys. Rev. B* **72**, 224429 (2005).
- <sup>27</sup>K. D. Usadel and U. Nowak, *Phys. Rev. B* **80**, 014418 (2009).
- <sup>28</sup>L. Del Bianco, D. Fiorani, A. M. Testa, E. Bonetti, and L. Signorini, *Phys. Rev. B* **70**, 052401 (2004).
- <sup>29</sup>H. Wang, T. Zhu, K. Zhao, W. N. Wang, C. S. Wang, Y. J. Wang, and W. S. Zhan, *Phys. Rev. B* **70**, 092409 (2004).